Flow and Transient Phenomena in Large Scale Additive Manufacturing.

Presenter: Eduardo Barocio,

Composites Additive Manufacturing Group
Composites Manufacturing and Simulation Center, Purdue University

FLOW PROCESSES IN COMPOSITE MATERIALS – 15

Agenda

- Large scale additive manufacturing
- Physics-based simulation workflow ADDITIVE3D for composites additive manufacturing
- Overview of physics considered
- Examples of simulation driven design with ADDITIVE3D
- Horizons and opportunities in composites additive manufacturing

Large Scale Additive Manufacturing (LSAM)

THERMWOOD LSAM RESEARCH LABORATORY

Workflow for Additive Manufacturing

CAD Geometry · Slicing · Printing

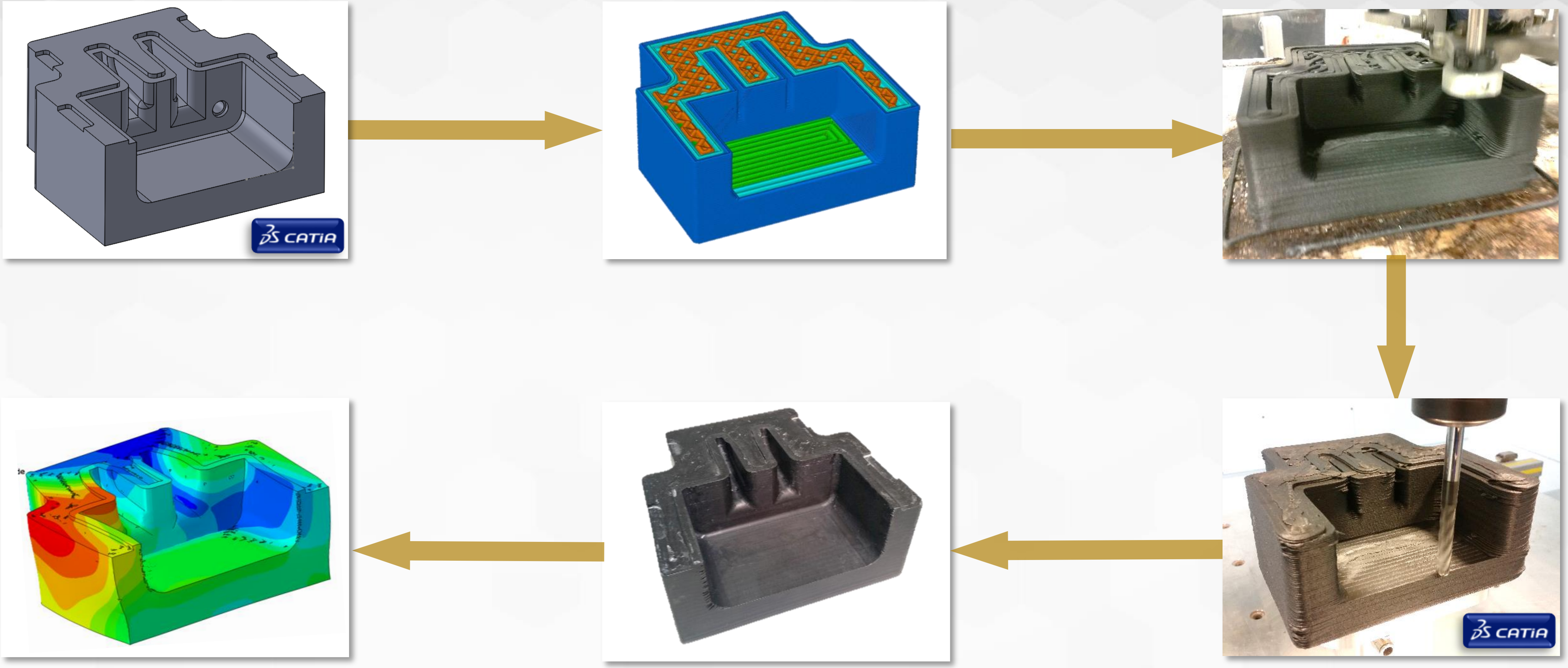

Performance · Final Part · Finishing

ADDITIVE3D: Simulation Workflow for AM

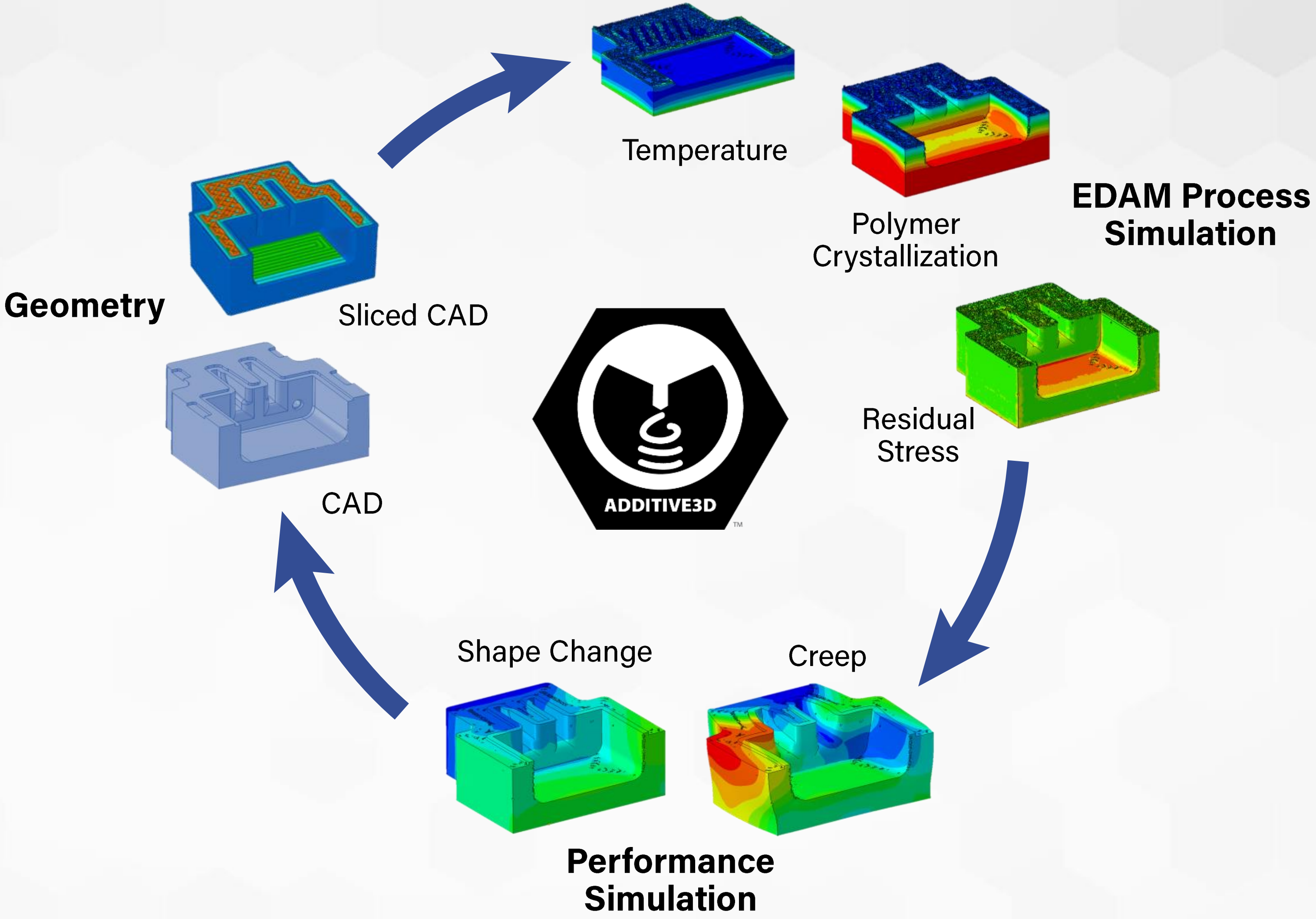

ADDITIVE3D™ Process and Performance Simulation

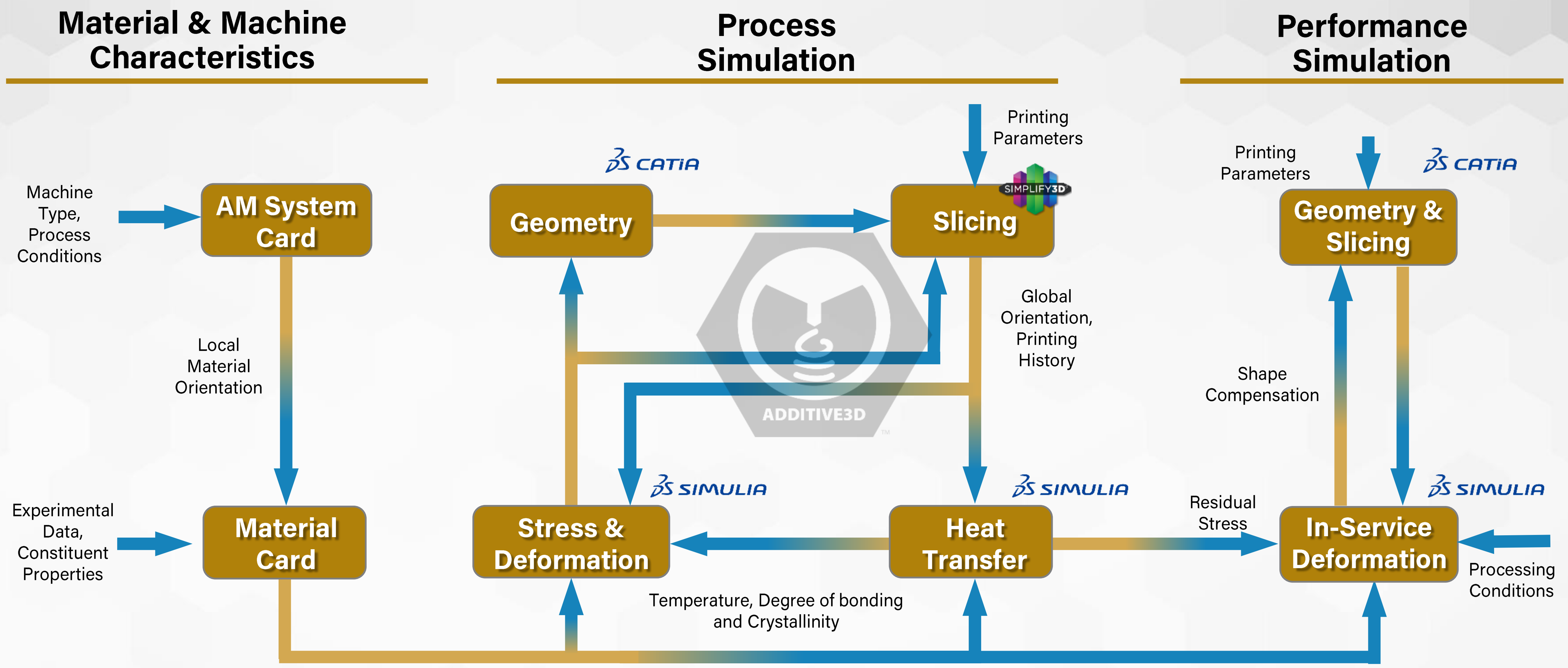

Physics Captured in AM Process Simulation

Multiscale and Multiphysics Process Simulations

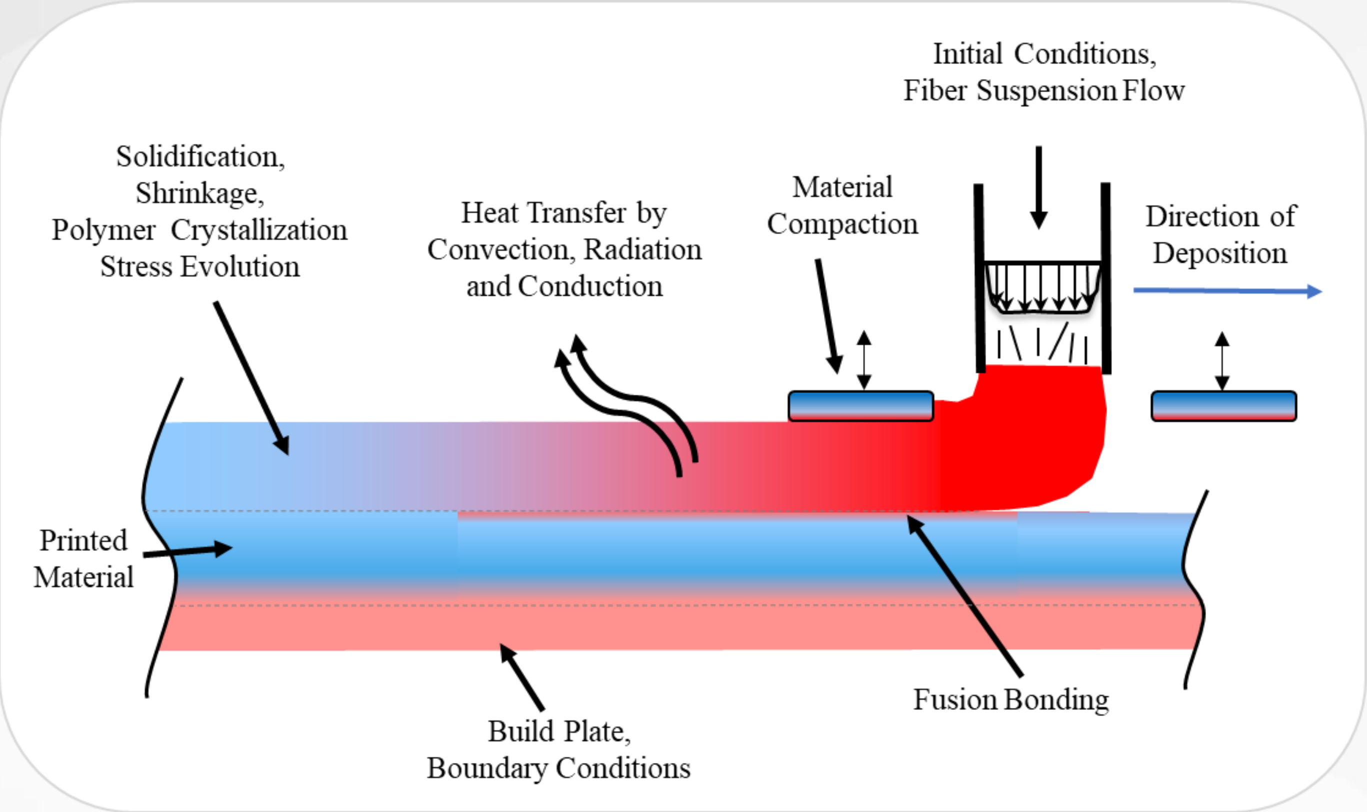

Barocio E, Brenken B, Favaloro A, Bogdanor M, Pipes RB. Extrusion Deposition Additive Manufacturing with Fiber-Reinforced Thermoplastic Polymers. In: Friedrich K, Walter R, editors. Struct. Prop. Addit. Manuf. Polym. Components. 1st ed., Woodhead Publishing; 2020, p. 450.

Inactive, Part-Unspecific Mesh

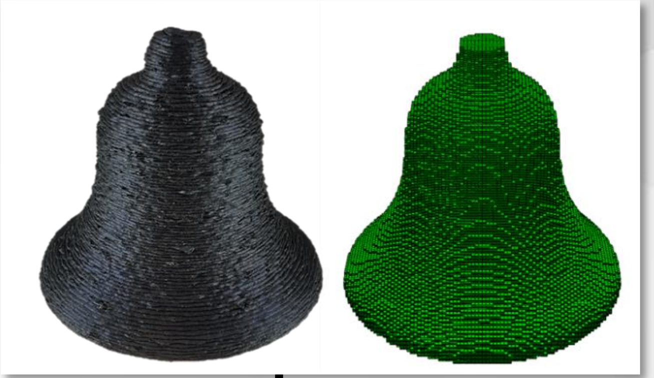

Element Activation Based on Machine Code

Anisotropic Flow of Fibers Polymer Suspension

Single Bead Deposition

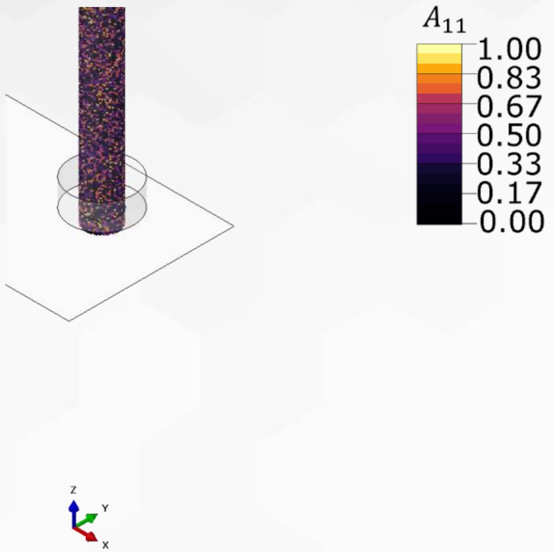

Single Bead Compaction

Second Bead Deposition

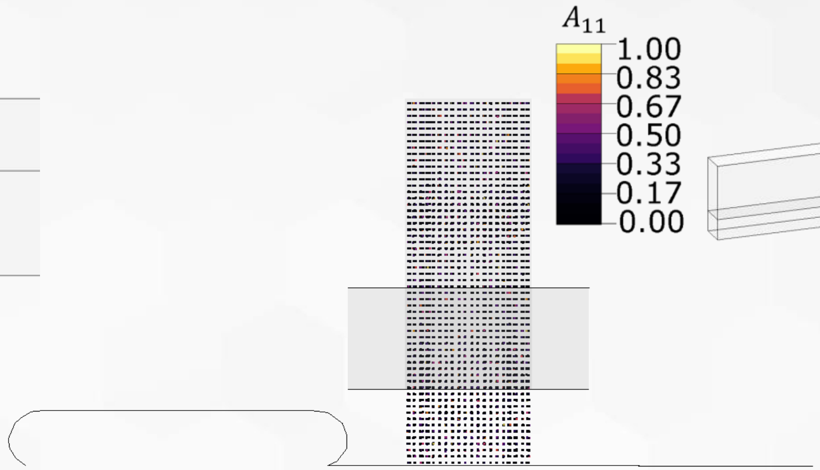

Second Bead Compaction

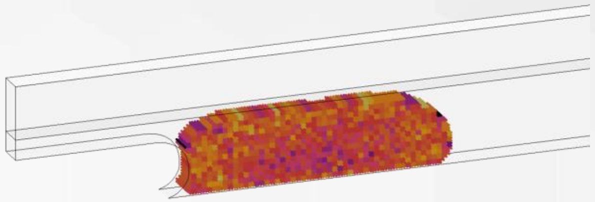

Pibulchinda P, Barocio E, Favaloro AJ, Pipes RB. Influence of printing conditions on the extrudate shape and fiber orientation in extrusion deposition additive manufacturing. Compos Part B Eng 2023;261:110793. https://doi.org/10.1016/j.compositesb.2023.110793.

Heat Losses in Material Compaction

- Actively cooled compacter
- Modeled as a moving heat flux with double gaussian distribution

$$q''(x,y,t) = \frac{Q^C\sqrt{AB}}{\pi} e^{-A(x+v_x t)^2} e^{-B(y+v_y t)^2}$$

- Tamper $A = B$
- Roller $A \neq B$

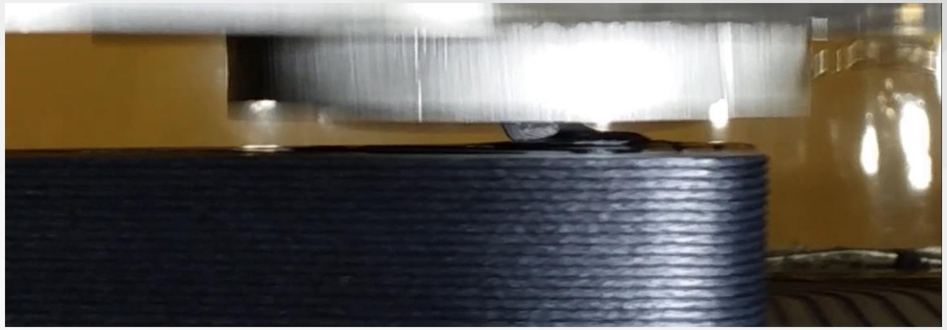

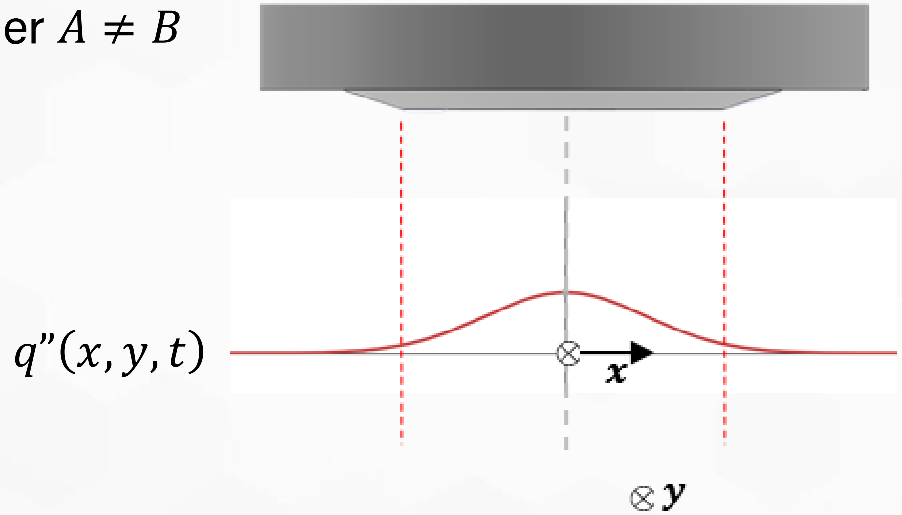

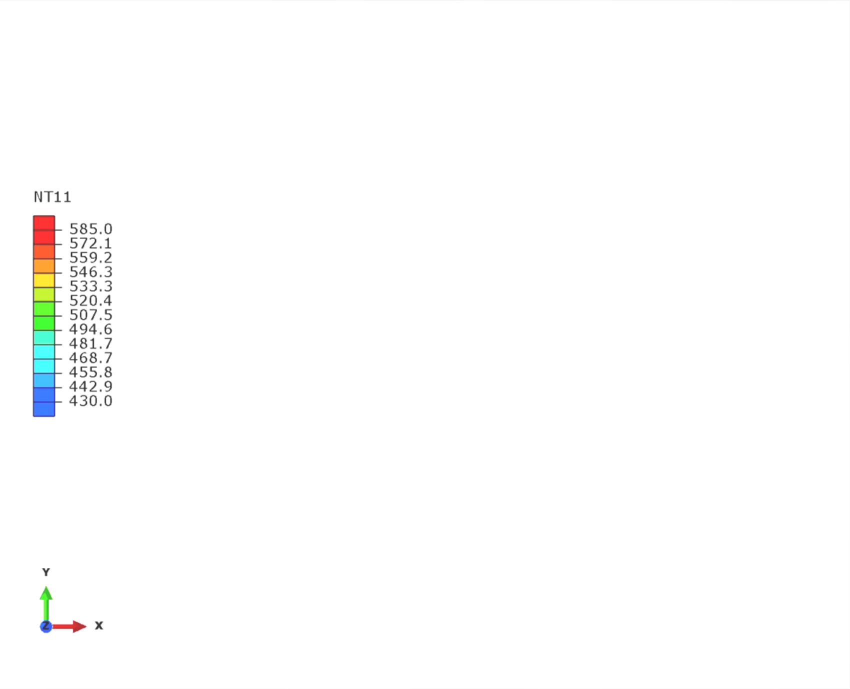

* Convection and radiation disabled

Local Convection Conditions

Feature dependent convection coefficients assumes:

- Convection occurs instantaneously
- Features are non-interactive
- Analogies made:
  - Solid section → Horizontal surface
  - External wall → Vertical surface
  - Internal wall and Infill section → Neglect or same as external wall

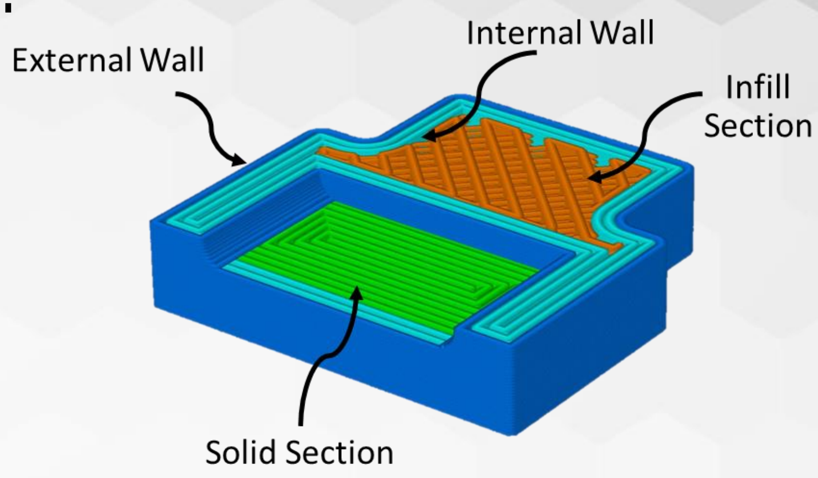

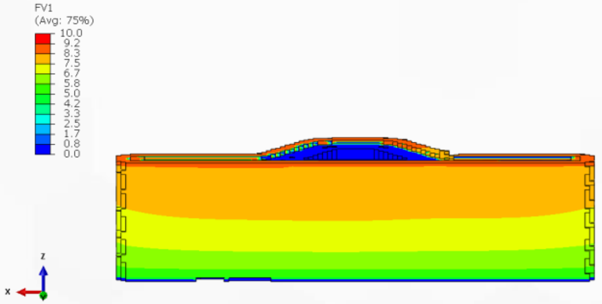

$t = 180\ s$

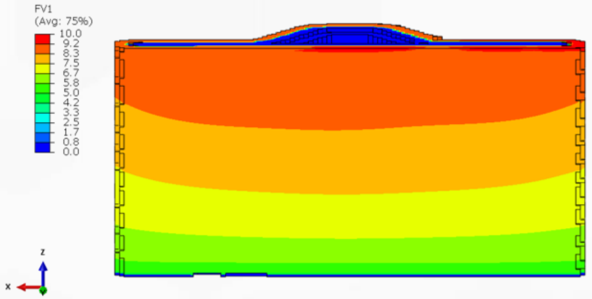

$t = 360\ s$

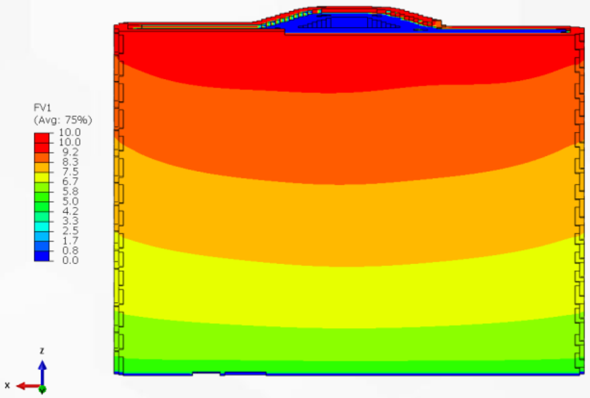

$t = 540\ s$

Convection coefficient at internal and external features

Polymer Crystallization Kinetics

- Polymer crystallization is cooling rate dependent
- Dual crystallization mechanisms observed in CF-PPS → Crystallization model developed by Velisaris and Seferis

$$X_{vc}(T,t) = X_{vc\infty}(w_1 F_{vc_1} + w_2 F_{vc_2})$$

$$F_{vc_i} = 1 - \exp[-C_{1_i} \int_0^t T \cdot exp\left[\frac{-C_{2_i}}{(T-T_g+T_{c_i})} - \frac{C_{3_i}}{\left(T\left(T_{m_i}-T\right)^2\right)}\right] n_i \tau^{n_i-1} d\tau \quad i = 1,2$$

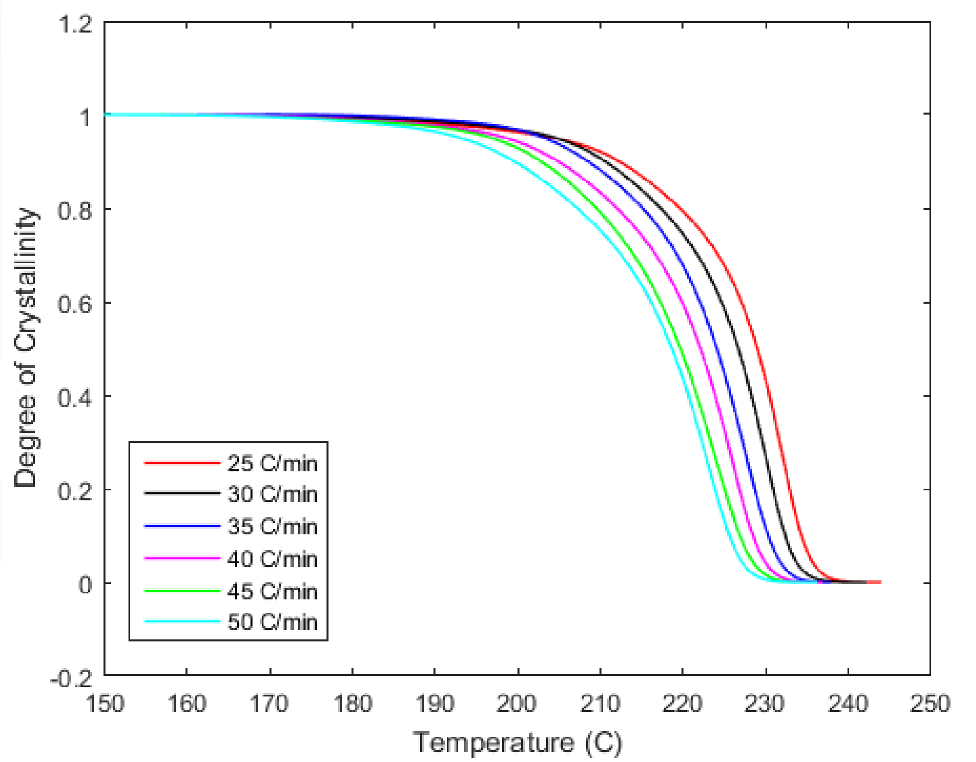

X_{vc} - crystallinity volume fraction, w_1 and w_2 are weight factors
C_{1_i} - pre-exponential factors capturing the temperature dependence
C_{2_i} - parameters associated with the temperature dependence of diffusion
C_{3_i} - parameters associated with the free enthalpy of nucleation
n_i - Avrami coefficients for each crystallization mechanism

Barocio E, Brenken B, Favaloro A, Bogdanor M, Pipes RB. Extrusion Deposition Additive Manufacturing with Fiber-Reinforced Thermoplastic Polymers. In: Friedrich K, Walter R, editors. Struct. Prop. Addit. Manuf. Polym. Components. 1st ed., Woodhead Publishing; 2020, p. 450.

Polymer Melting

- Melting model assumes statistical distribution of lamellar thicknesses (Greco & Maffezzoli) -> Only temperature dependent

$$T_m = T_m^\circ - \frac{2\gamma_e T_m^\circ}{l\Delta H_f}$$

$$\frac{dX_{vc}}{dT} = k_{mb}\{exp^{[-k_{mb}(T-T_c)]}\} \cdot \left(1 + (d-1)exp^{[-k_{mb}(T-T_c)]}\right)^{\frac{d}{1-d}}$$

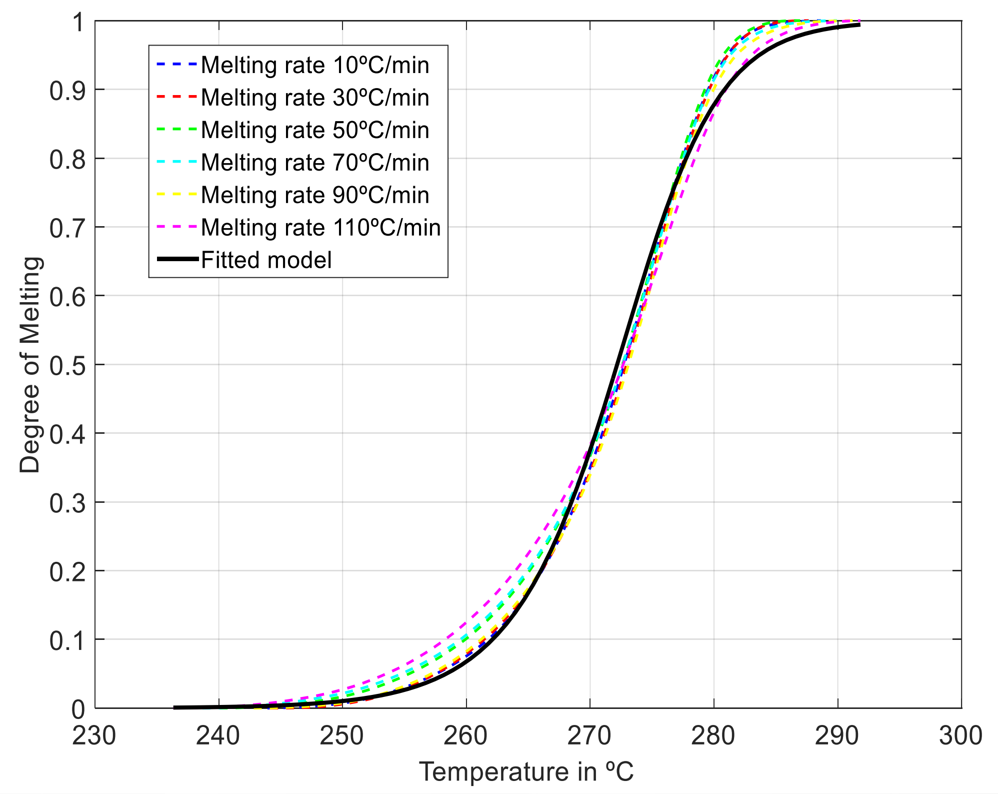

T_c - crystallization temperature
k_{mb} - sharpness of the distribution of lamellar thicknesses
d - shape factor of the distribution of lamellar thicknesses

γ_e - lateral surface energy
T_m°- thermodynamic melting temperature
ΔH_f - enthalpy of fusion
l - lamellar thickness

Barocio E, Brenken B, Favaloro A, Bogdanor M, Pipes RB. Extrusion Deposition Additive Manufacturing with Fiber-Reinforced Thermoplastic Polymers. In: Friedrich K, Walter R, editors. Struct. Prop. Addit. Manuf. Polym. Components. 1st ed., Woodhead Publishing; 2020, p. 450.

Thermoviscoelastic Material Behavior

Anisotropic linear constitutive equation:

$$\sigma_i = \int_0^t C_{ij}(T, X, t-\tau) \frac{\partial \varepsilon_j^{eff}}{\partial \tau} d\tau , \qquad i,j = 1,2,\ldots 6$$

T: Temperature, X: Crystallinity, t: Time

$\varepsilon_j^{eff} = \varepsilon_j - \varepsilon_j^{inel}$: Effective strain

Time-Temperature-Superposition (TTS):

$$\xi_{ij}(t) = \int_0^t \frac{1}{a_T(T(\tau))} d\tau$$

$\xi_{ij}(t)$: Reduced time, $a_T(T)$: Shift factor (WLF Equation)

$$C_{ij}\left(T_0, X, \xi_{ij}(t) - \xi'_{ij}(\tau)\right) = f(X) \cdot \left[C_{ij0} + \sum_{w=1}^{N} C_{ijw} \exp\left(-\frac{\xi_{ij}(t) - \xi'_{ij}(\tau)}{\lambda_{ijw}}\right)\right]$$

λ_{ijw}: Relaxation times

$f(X)$: Crystallization factor

C_{ij0}, C_{ijw}: Relaxed/Unrelaxed stiffness parts

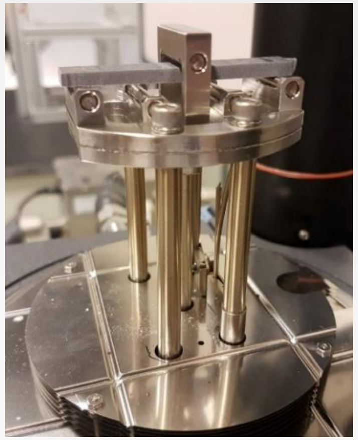

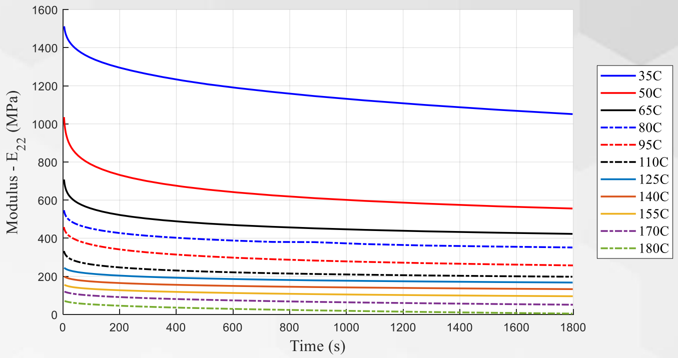

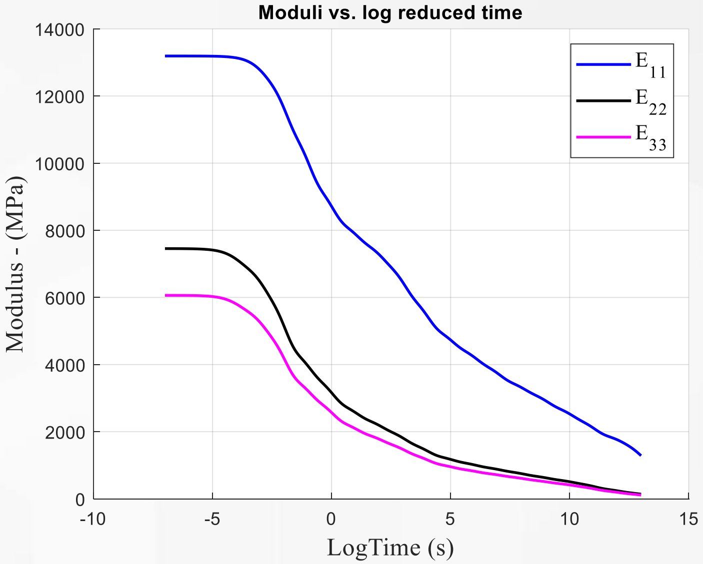

Brenken B, Favaloro A, Barocio E, Kunc V, Pipes RB. Thermoviscoelasticity in extrusion deposition additive manufacturing process simulations. 32nd Tech. Conf. Am. Soc. Compos. 2017, vol. 1, 2017.

Anisotropic Shrinkage

- Contribution from both thermoelastic and crystallization shrinkage
- Thermoelastic shrinkage: Governed by $\alpha(T)$
- Strain developed before crystallization does not contribute significantly to build up stresses

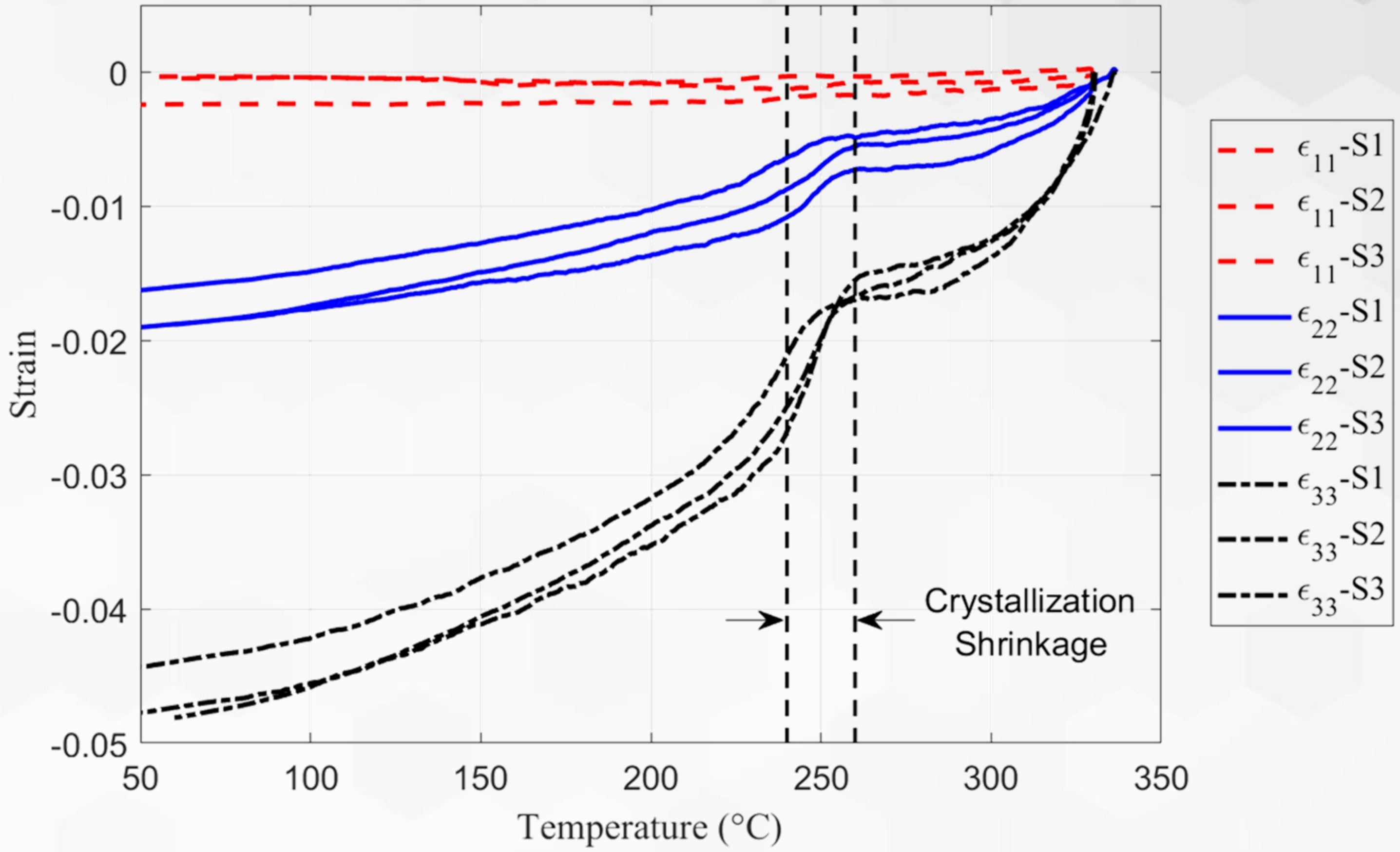

Barocio E, Brenken B, Favaloro A, Bogdanor M, Pipes RB. Extrusion Deposition Additive Manufacturing with Fiber-Reinforced Thermoplastic Polymers. In: Friedrich K, Walter R, editors. Struct. Prop. Addit. Manuf. Polym. Components. 1st ed., Woodhead Publishing; 2020, p. 450.

Interlayer and Fusion Bonding

- Non-isothermal fusion bonding model provides prediction of fracture properties
- Integrates effect of polymer crystallization on precluding reptation of polymer chains
- Model extended to inter-bead fusion bonding

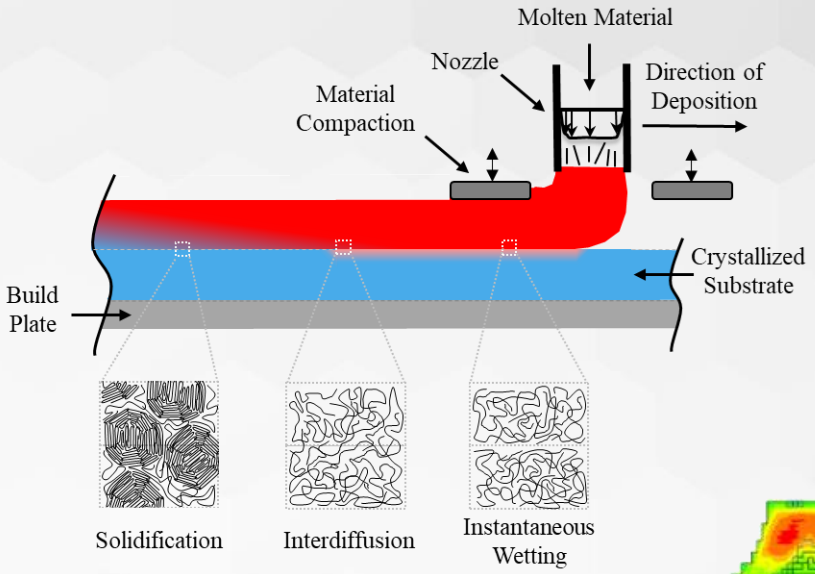

$$D_b(t) = \frac{G_{1C}(t)}{G_{1C\infty}} = \left[\int_0^{t_c} \frac{1}{t_w(T(\tau))} d\tau\right]^{\frac{1}{2}}, t_c \in \{t\ s.t.\ X_{vc} < X_{vc}^{crit}\}$$

$$t_w(T(\tau)) = A \cdot exp\left(\frac{E_A}{RT(\tau)}\right)$$

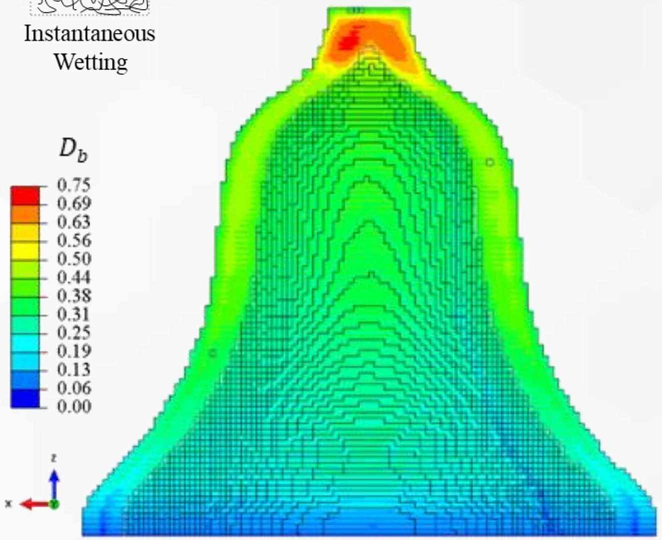

t_w - welding time
E_A - activation energy
A - pre-exponential factor
$G_{1C\infty}$ - critical energy release rate of a perfectly bonded interface

Barocio E, Brenken B, Favaloro A, Pipes RB. Interlayer fusion bonding of semi-crystalline polymer composites in extrusion deposition additive manufacturing. Compos Sci Technol 2022:109334. https://doi.org/10.1016/j.compscitech.2022.109334.

Interaction with Print Substrate

Adhesive / Beadboard

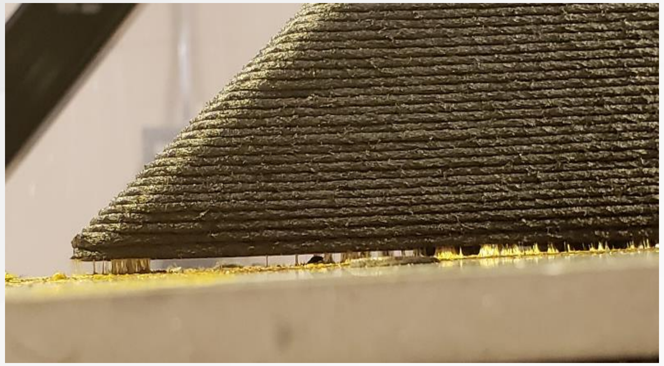

Boundary Conditions

Thermal

$q_s^{"} = 0 \;|\; T_s = T_{bp} \;|\; R_\theta$

Mechanical

Cohesive Contact

$\mathrm{t_n}(\delta_1, D), \mathrm{t_s}(\delta_s, D), \mathrm{t_t}(\delta_t, D)$

Build Sheets

Boundary Conditions

Thermal

$T_{bs} = T_{bp} \;|\; R_\theta$

Mechanical

Spring Connectors

$F_i = F_i^0 + \cancel{D_{ij} u_j}$

Rigid Constraint

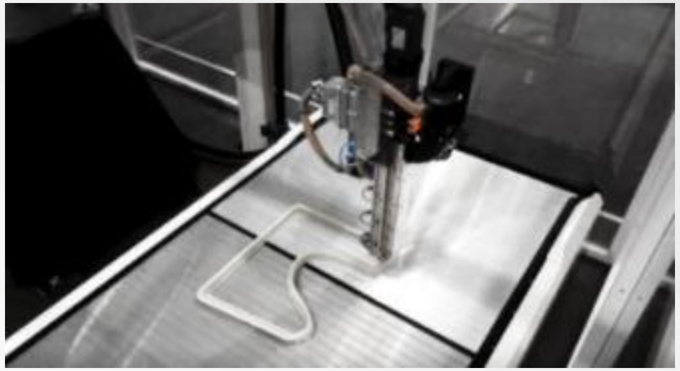

Boundary Conditions

Thermal

$T_s = T_{bp} \;|\; R_\theta$

Mechanical

All DOF Constrained

$u_i = 0$

Barocio E, Thomas AJ, Pipes RB. Virtual Investigation of Residual Part Deformation Due to Build Plate Support Characteristics in Material Extrusion Additive Manufacturing. CAMX 2020 – Compos. Adv. Mater. Expo, VIRTUAL EXPERIENCE: CAMX 2020; 2020.

Material Card Characterization

Bead-Level Effective Properties

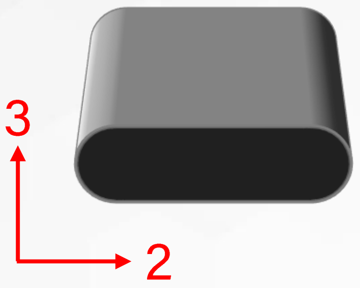

Material Property	Relevant Standard
Glass Transition Temperature	ASTM D7028
Fiber Orientation Distribution	
Fiber Length Distribution	
Elastic Properties (9 components)	ASTM D3039 ASTM D5379
Coefficient of Thermal Expansion (3 directions)	ASTM E831
Crystallization Kinetics and Melting	
Thermoviscoelastic Behavior (9 Prony series)	ASTM D5023
Thermal Conductivity (3 directions)	ASTM E1461
Heat Capacity	ASTM E1269
Fusion Bonding Time	

Material Card Generation

User Input

Experimental Characterization

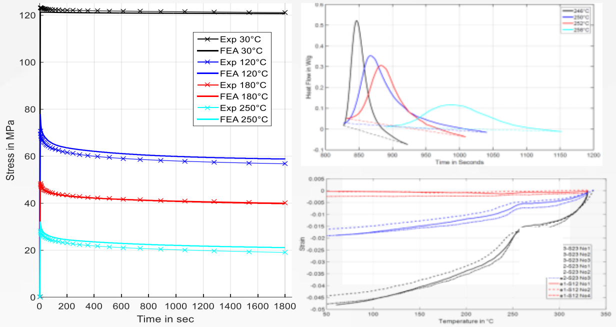

Experimental Data

AM System Card

LSAM
Large Scale Additive Manufacturing
CAMRI
Composites Additive Manufacturing Research Instrument
TITAN ROBOTICS LTD.
CI BAAM
⋮

Constituent Properties,
Homogenized Properties

Bead Geometry
Local Fiber Orientation,

Material Card Generation

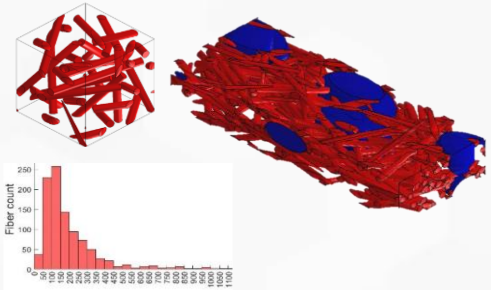

Property Prediction

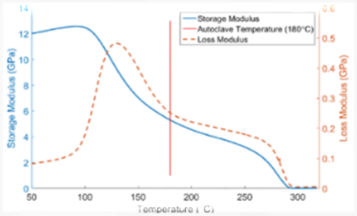

Material Models

Digital Material Card

Accelerating Material Card Generation

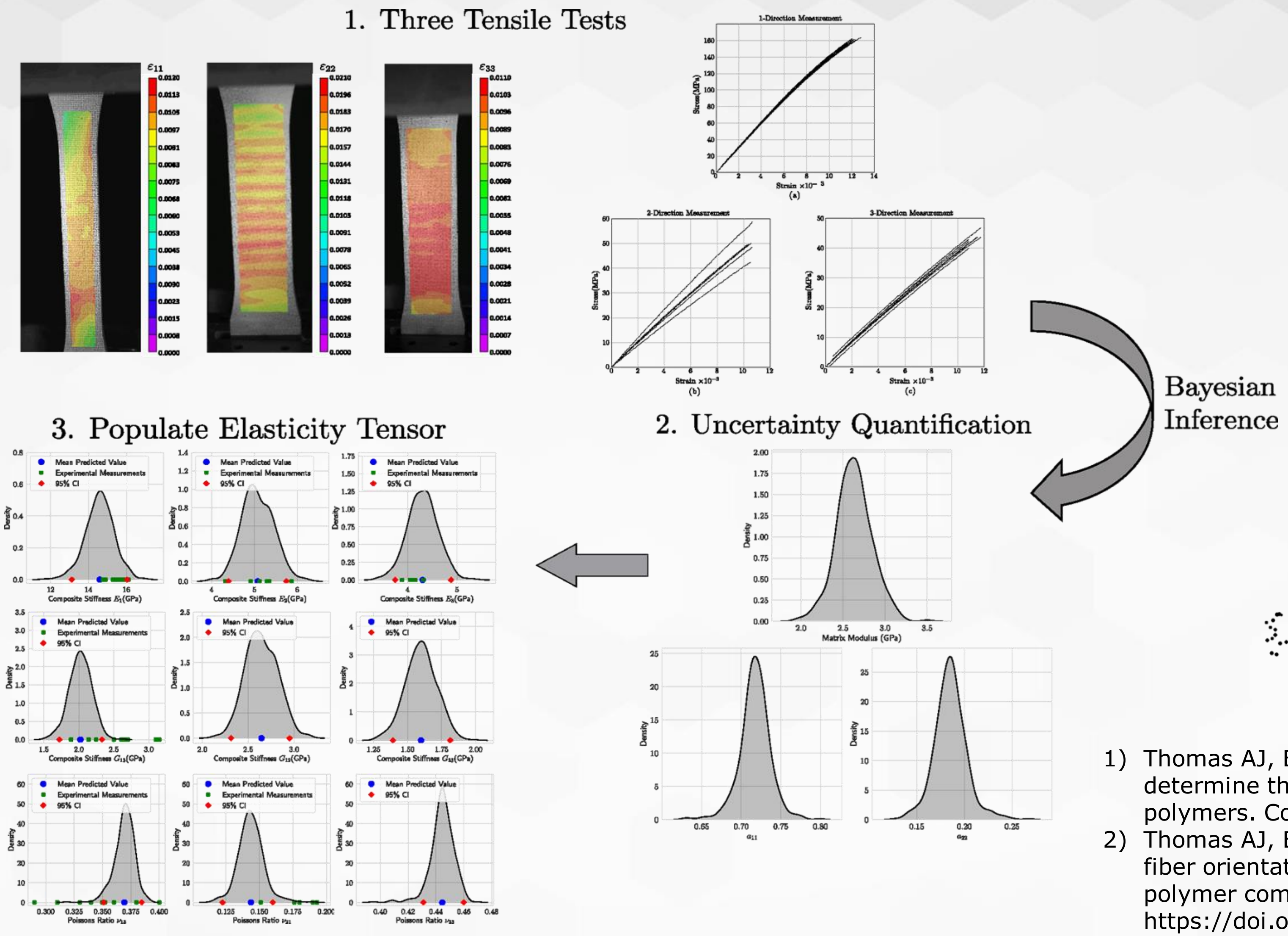

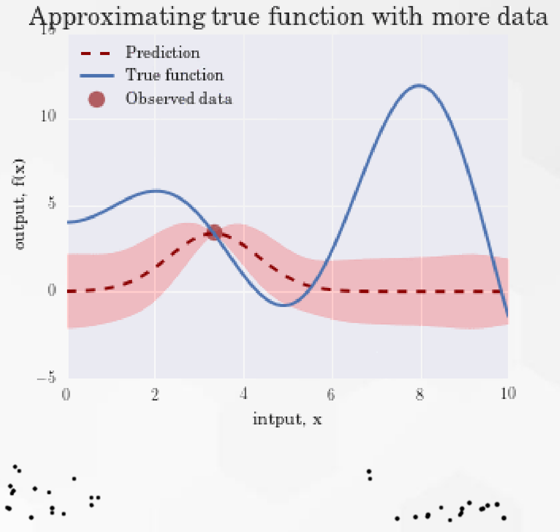

1) Thomas AJ, Barocio E, Pipes RB. A machine learning approach to determine the elastic properties of printed fiber-reinforced polymers. Compos Sci Technol 2022:109293.
2) Thomas AJ, Barocio E, Bilionis I, Pipes RB. Bayesian inference of fiber orientation and polymer properties in short fiber-reinforced polymer composites. Compos Sci Technol 2022;228:109630. https://doi.org/10.1016/j.compscitech.2022.109630.

Transferring Material Cards Across AM Systems

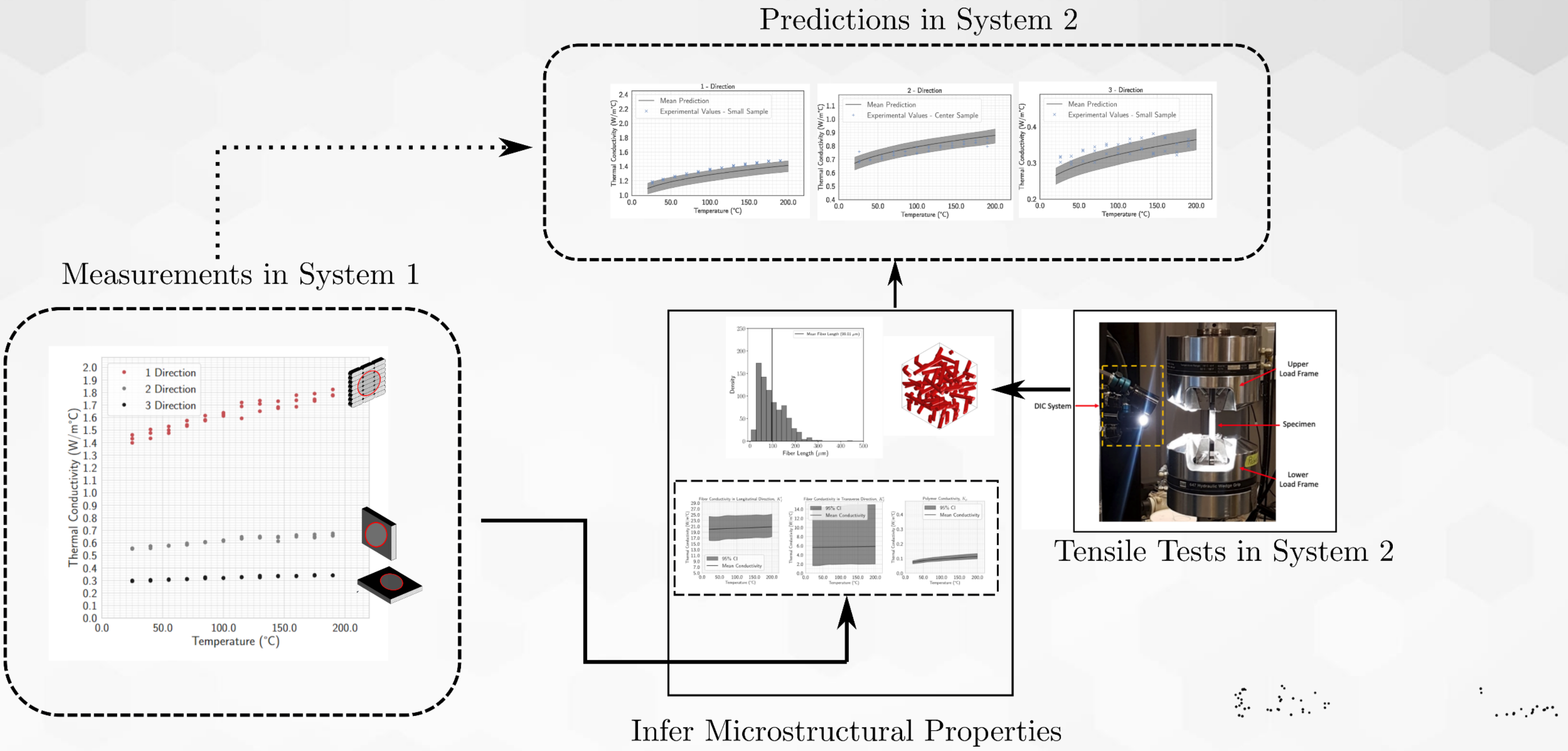

Machine Card Characterization

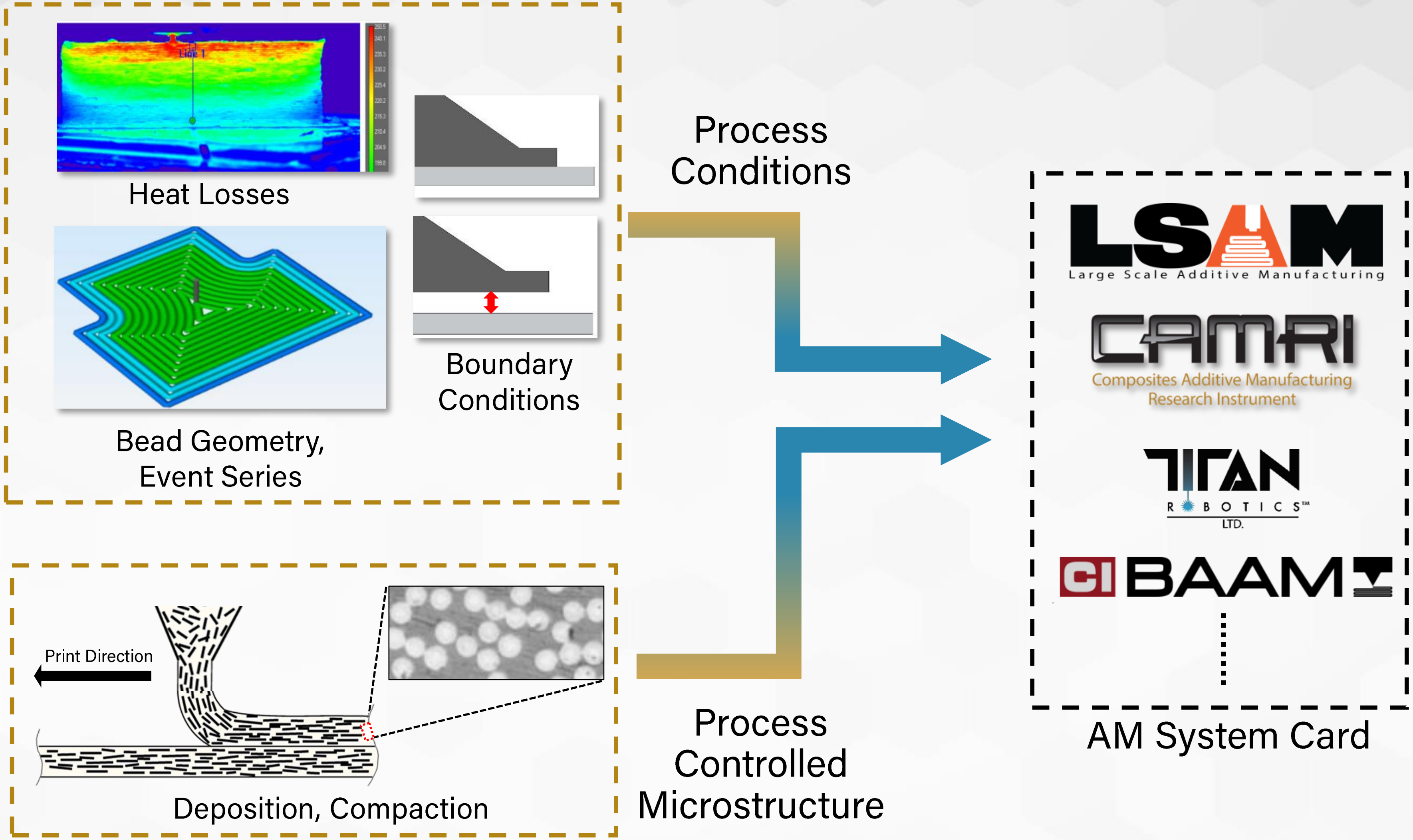

Simulation Driven Design with ADDITIVE3D

Simulation-Driven Shape Compensation of Autoclave Tool

Nominal Geometry

Process Simulation

ADDITIVE3D™

Post-Printing Geometry

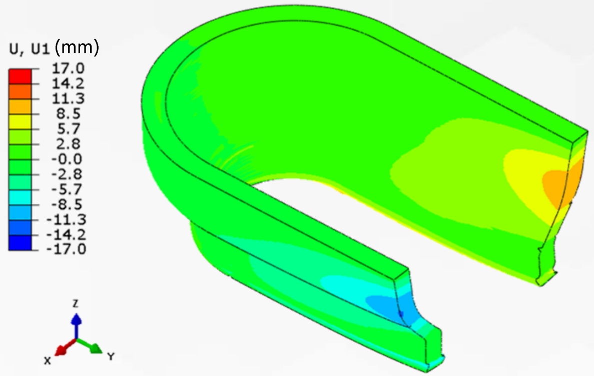

Shape Compensation

Compensated Geometry

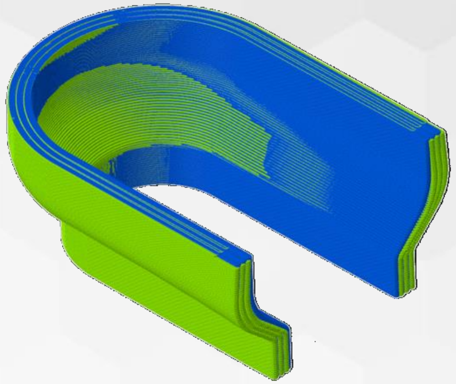

Removal of Printed Geometry

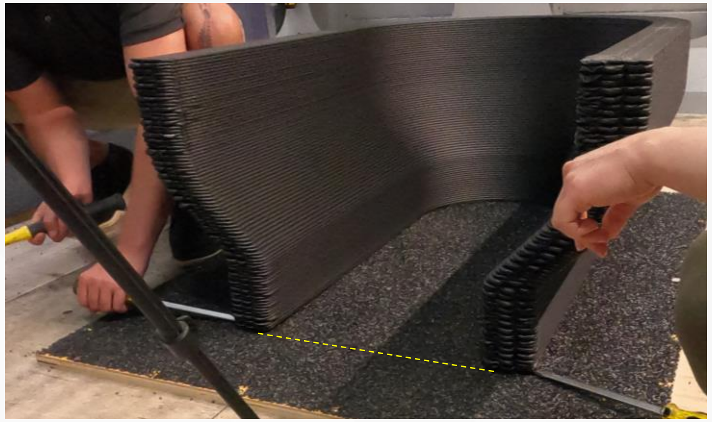

Printing

Validation

Printed vs Nominal Geometry

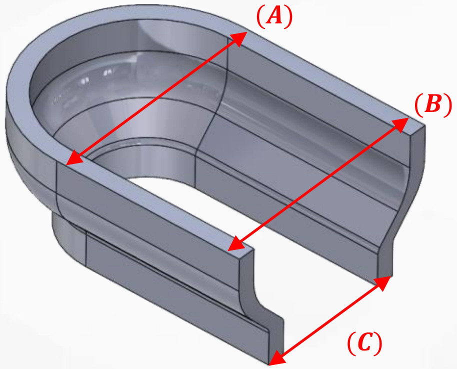

Location	Nominal vs Printed Geometry (mm)
A	0.71
B	1.01
C	0.89

Reduction of Part Deformation Driven by Analysis

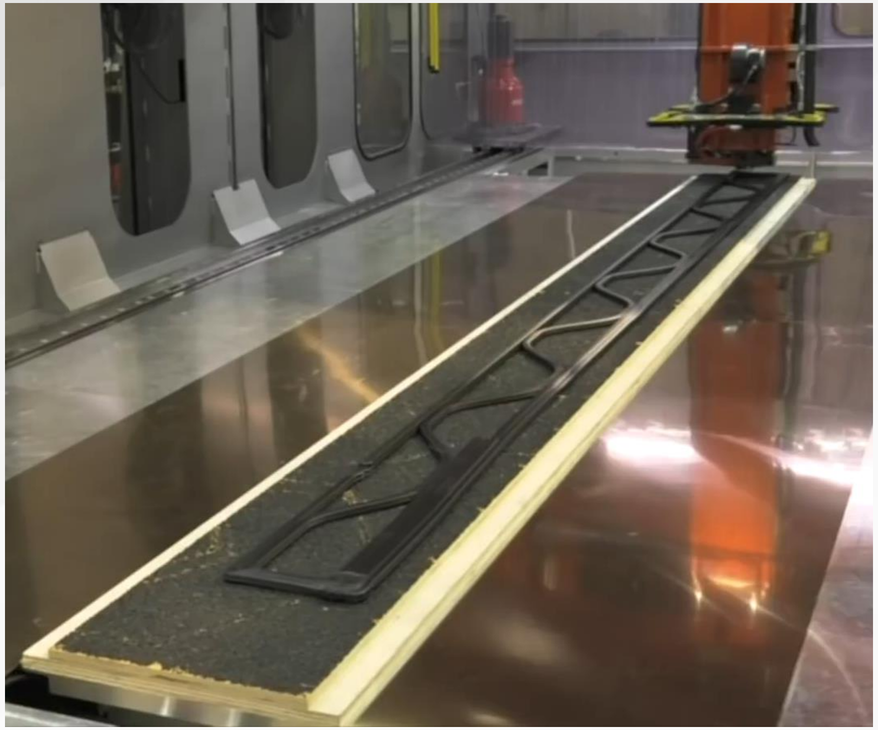

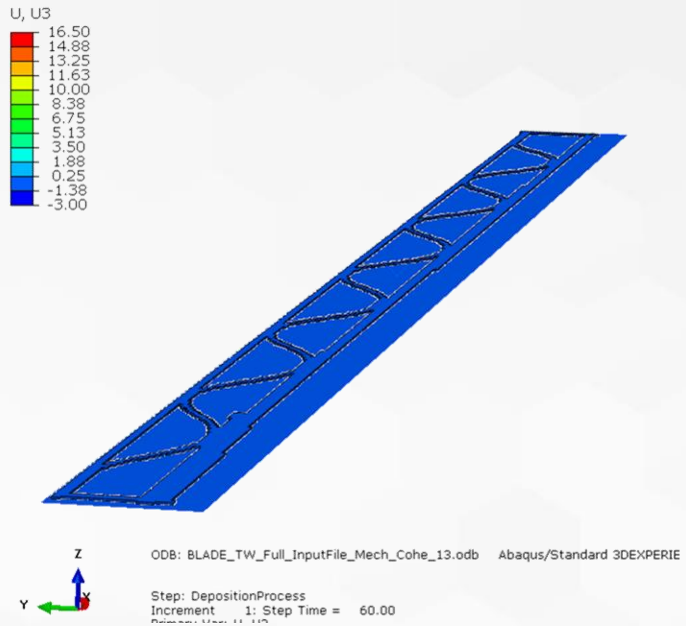

- Autoclave tool made from Techmer PM Electrafil® PESU 1810 3DP
- Three failed print iterations utilizing ~1,500lb each -> ~75% savings.
- ADDITIVE3D simulations utilized after multiple failures to drive success on the final print.

Structural Analysis of Printed Torch

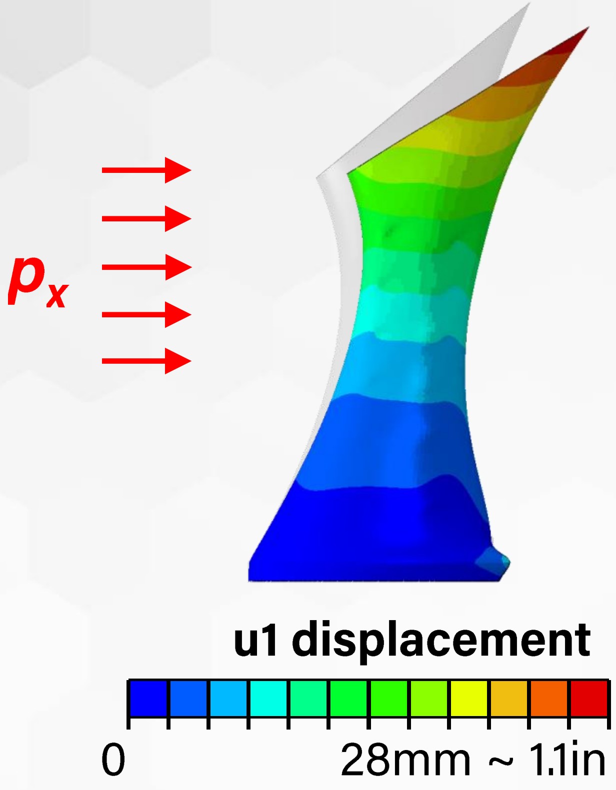

- Structural analysis to quantify displacement under load
- Risk assessment to ensure structural integrity

ADDITIVE3D for "First time right printing"

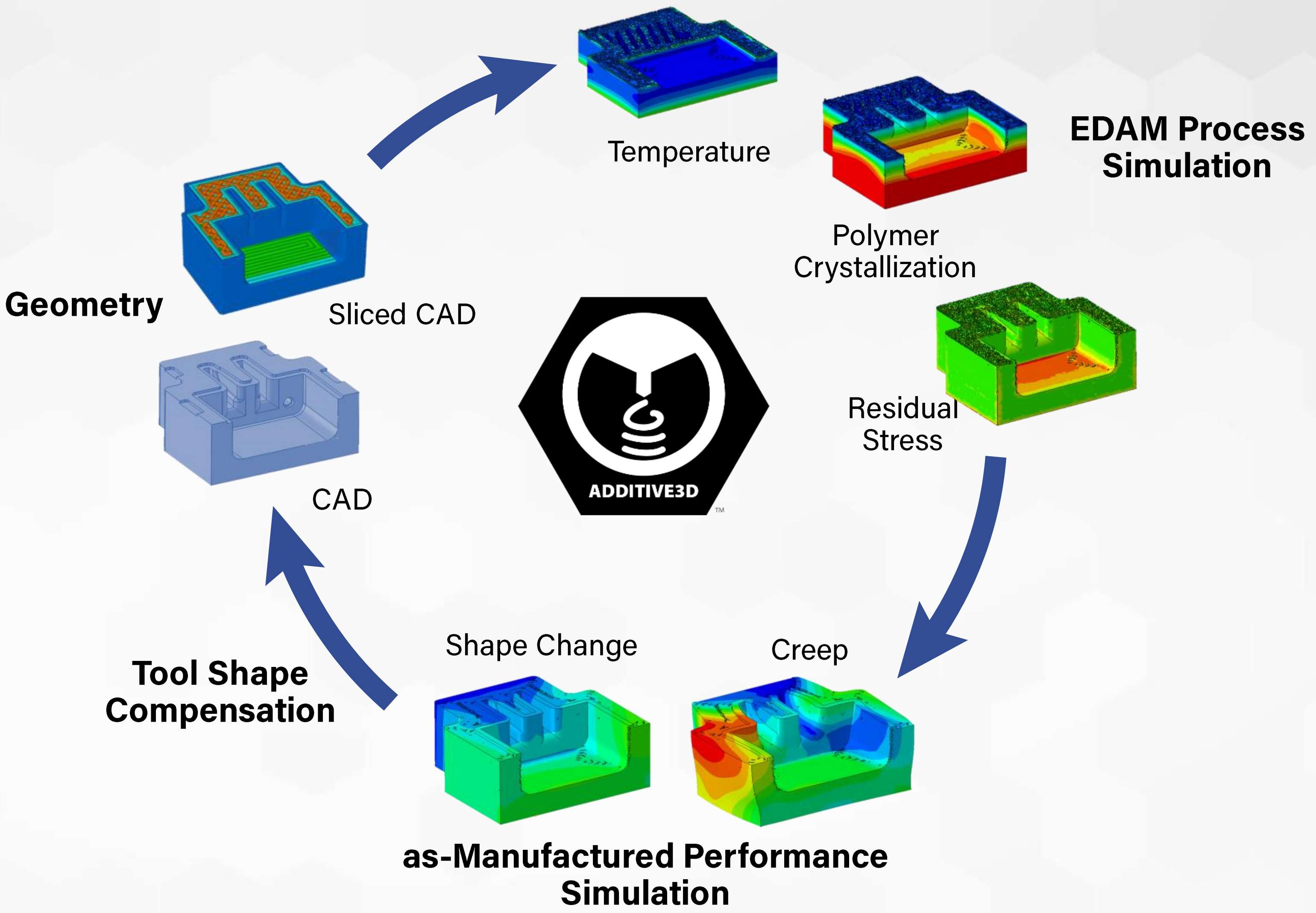

Horizons and Opportunities in Composites Additive Manufacturing

Printing of Hybrid Continuous and Discontinuous Fiber Systems

- Opportunity
  - Elevate the large-scale additive manufacturing process to produce semi-structural components
  - Printing rates similar to large scale additive manufacturing with short fiber reinforced polymers are possible
  - Selective printing of continuous and discontinuous fibers
  - Integration of sensors and services (heating) in continuous fibers
- Process demonstrated in the CAMRI system at Purdue with continuous fiber filament impregnated in house (AS4 – PPS)

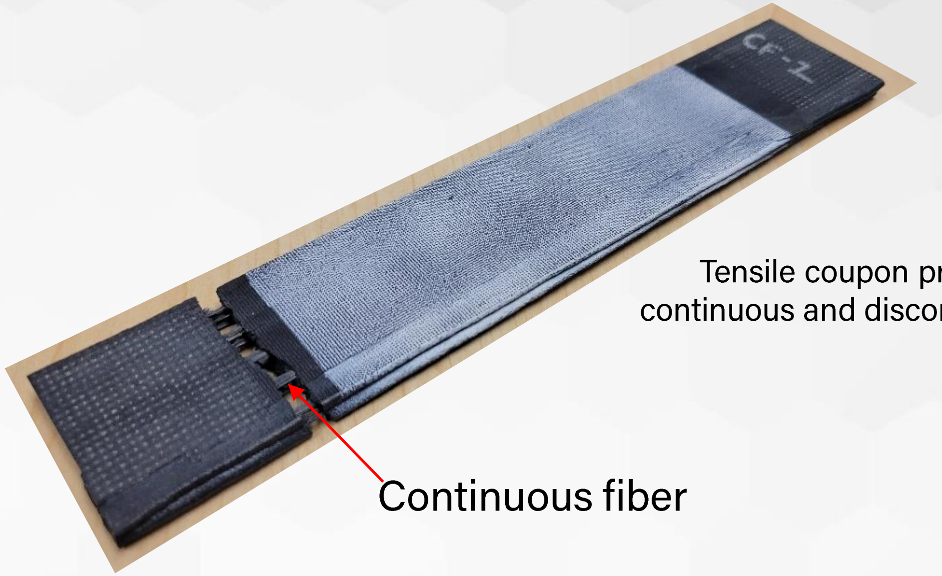

Tensile coupon printed with continuous and discontinuous fibers

US011214006B2

(12) **United States Patent**
Barocio et al.

(10) **Patent No.:** US 11,214,006 B2
(45) **Date of Patent:** Jan. 4, 2022

(54) METHODS AND APPARATUS FOR ADDITIVE MANUFACTURING UTILIZING MULTIFUNCTIONAL COMPOSITE MATERIALS, AND ARTICLES MADE THEREFROM

(58) **Field of Classification Search**
CPC ... B29C 64/336; B29C 64/118; B29C 64/209; B33Y 10/00; B33Y 30/00; B33Y 40/00; B33Y 70/00
See application file for complete search history.

Printing of Continuous and Discontinuous Fibers

- Fundamental problems to investigate:
  - Concurrent flow of continuous and discontinuous fibers from nozzle to deposition
  - Adhesion between continuous and discontinuous fiber systems
  - Optimal microstructures for load transfer
  - Strength characteristics of hybrid printed materials
  - Design for printing with hybrid continuous and discontinuous fibers

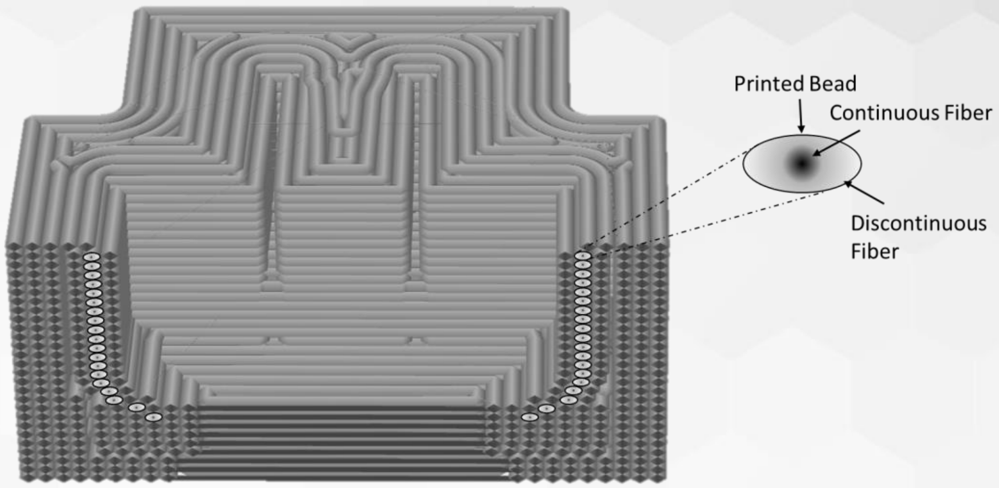

Compression molding tool concept printed with continuous and discontinuous fibers

Compression Molding of SMC and Printed Continuous Fiber Preforms

- Opportunity
  - Increase strength characteristics of compression molded components
  - Reduce variability in strength characteristics which elevates design allowables for this class of material systems
  - Elevate value of recycled material (upcycle) with the addition of a small fraction of continuous fiber printed preforms
- Initial demonstration of the potential for this technology through a pin bracket geometry in collaboration with 9T LABS

Initial Continuous Fiber Preform Configuration

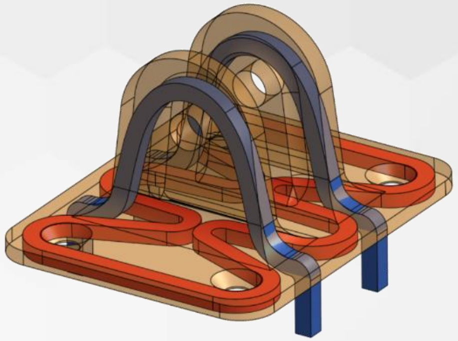

Expected Continuous Fiber Configuration after Flow

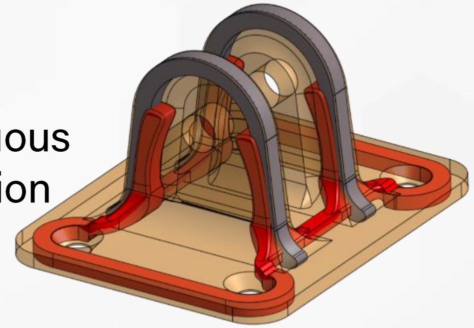

CT-Scan of Bracket Molded with Hybrid Material System

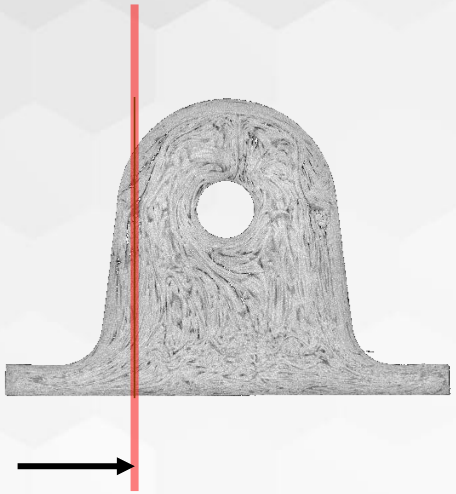

Hybrid Platelet
+
CF Preform

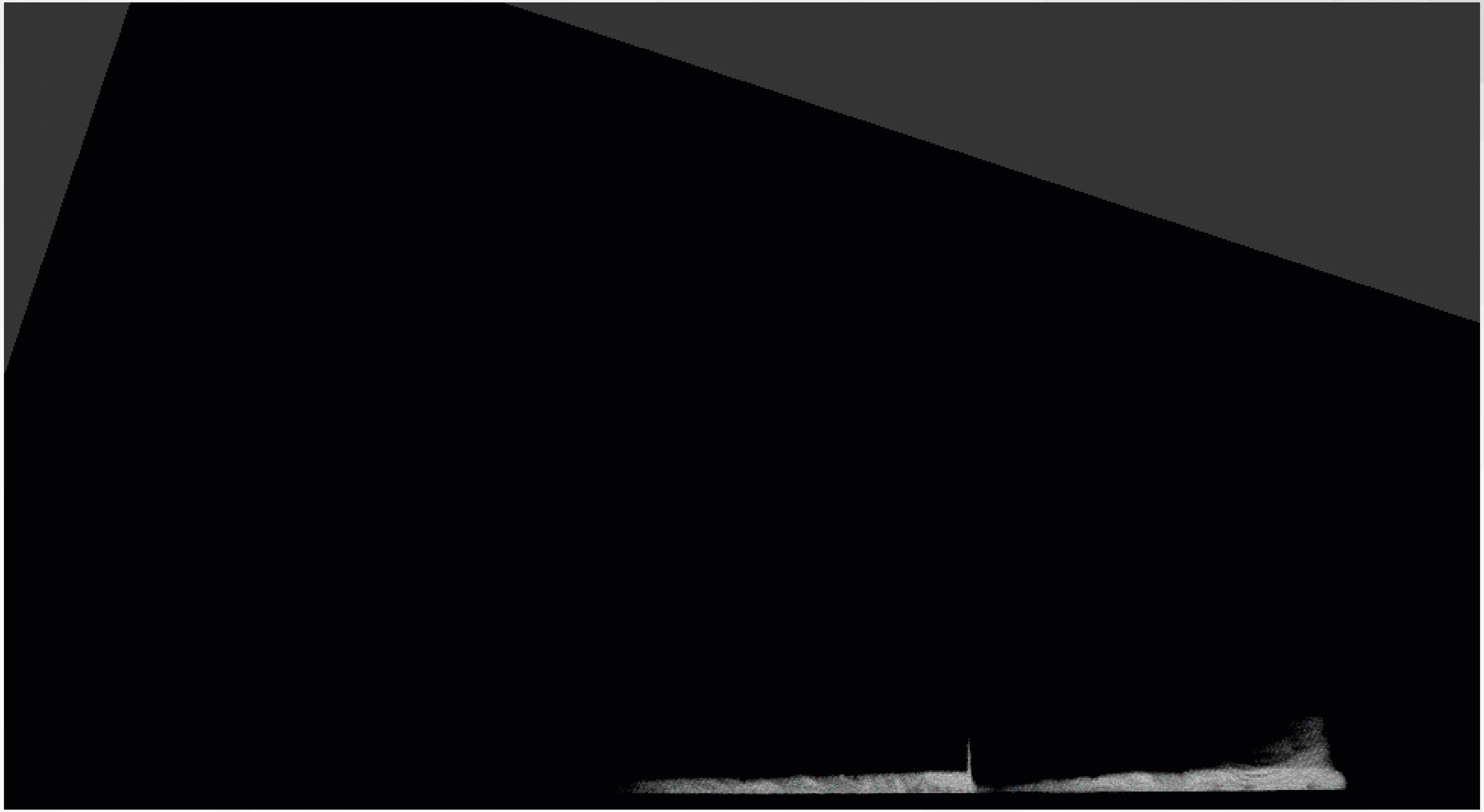

CT-Scan of Bracket Molded with Hybrid Material System

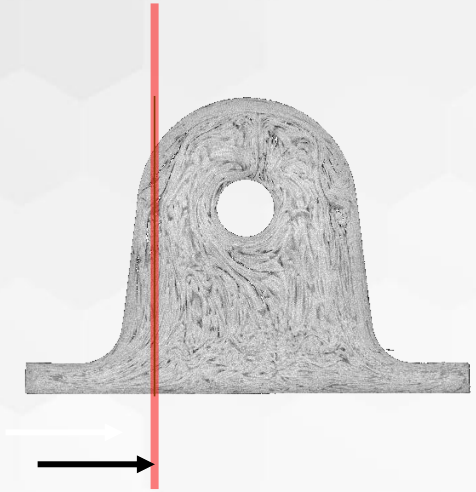

Hybrid Platelet
+
CF Preform

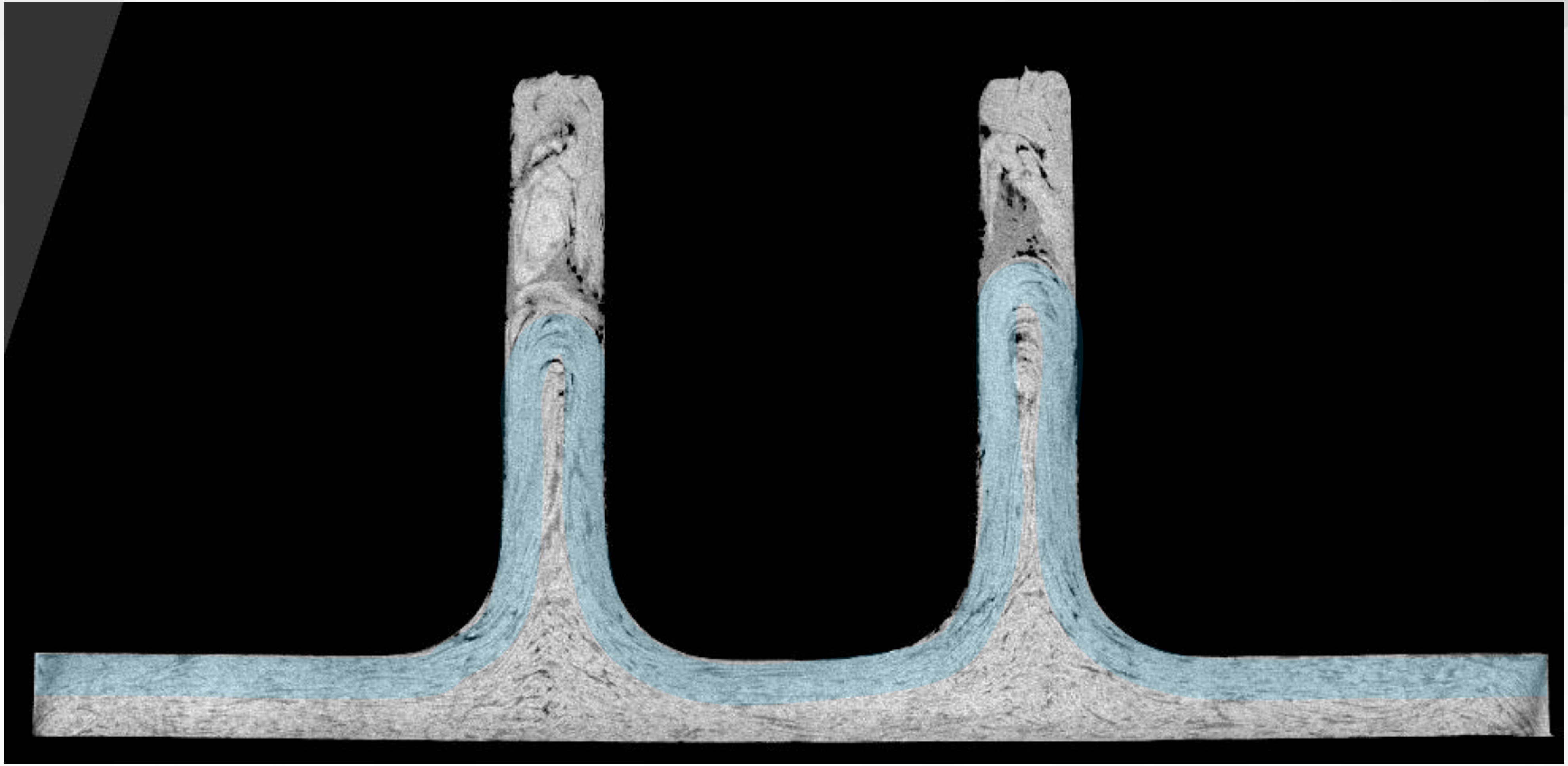

Structural Performance of Hybrid Material System

Hybrid
SMC
+
CF
Preform

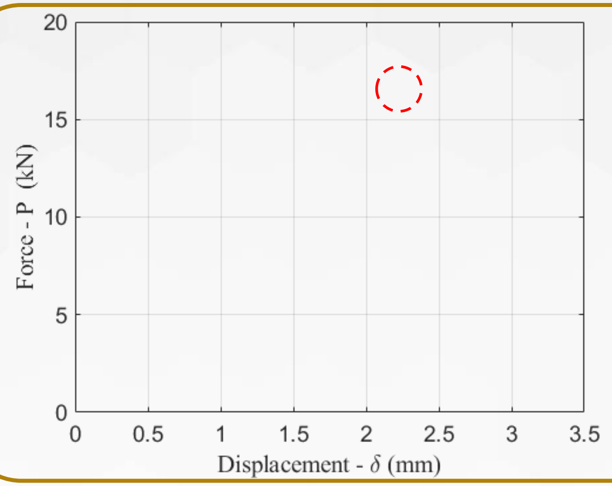

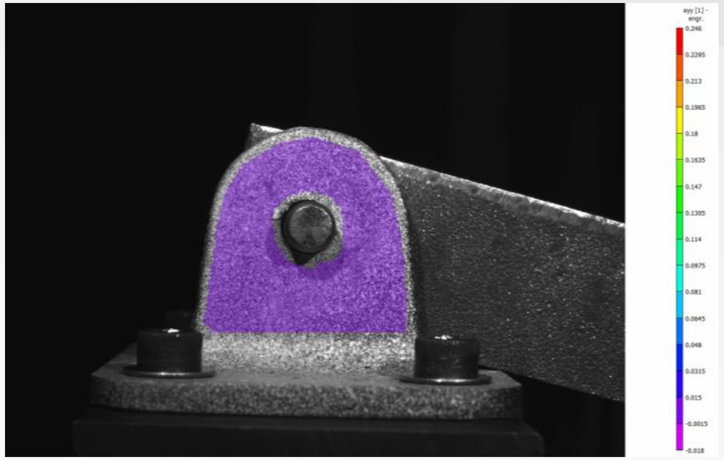

SMC

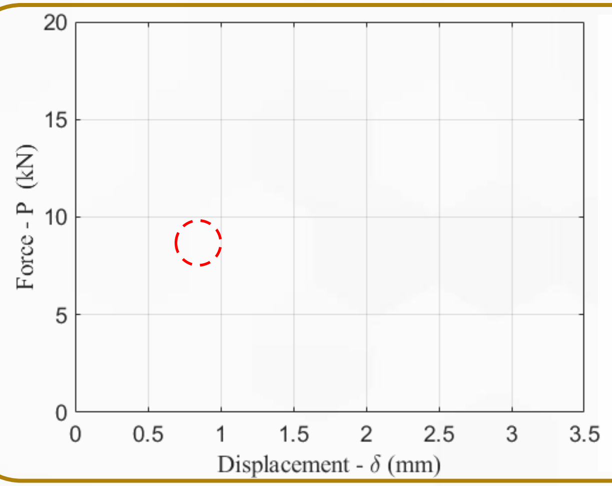

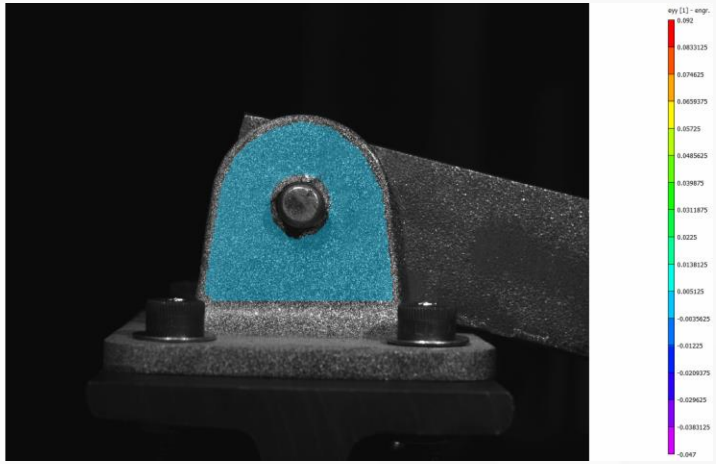

Barocio E, Eichenhofer M, Kalman J, Fjeld LM, Kirchhoff J, Kim G, et al. Compression Molding of Hybrid Continuous and Discontinuous Fiber Reinforced Thermoplastics for Enhancing Strength Characteristics. SAMPE Conf., Seattle, WA: SAMPE; 2023.

Compression Molding of Continuous and Discontinuous Fibers

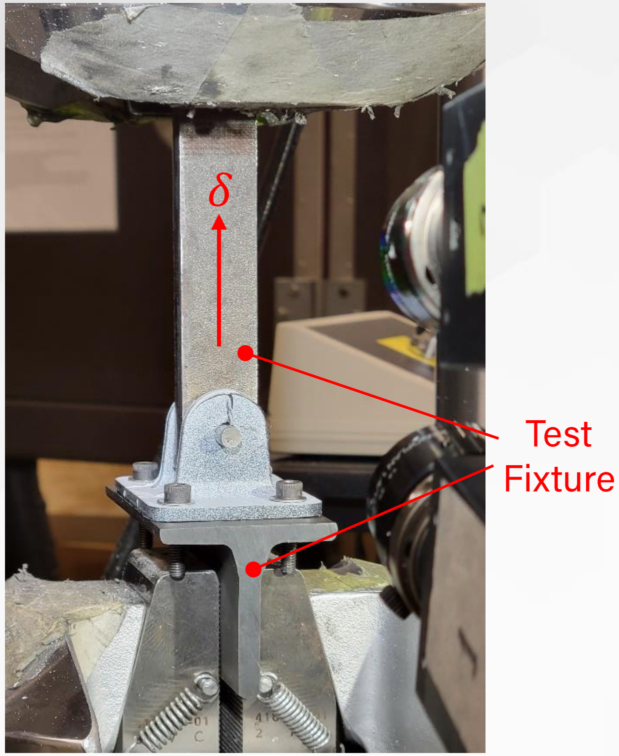

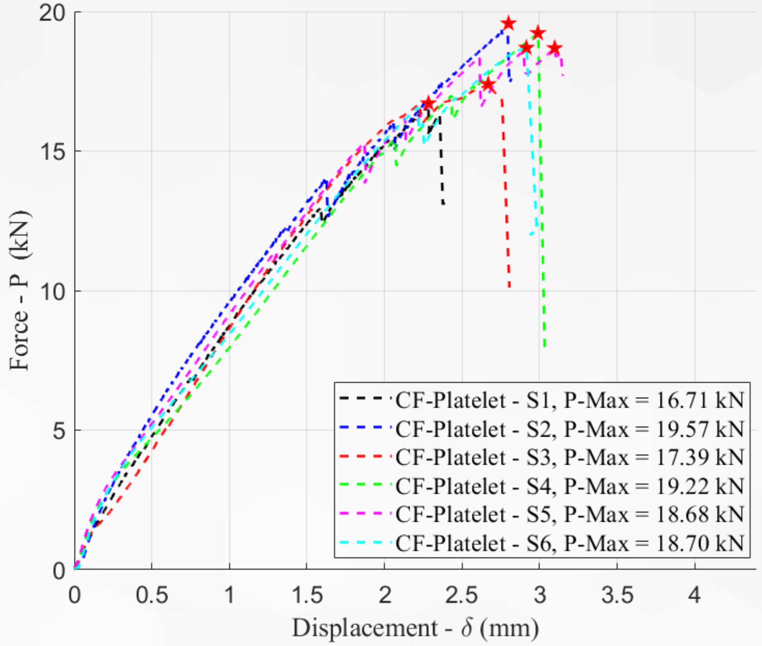

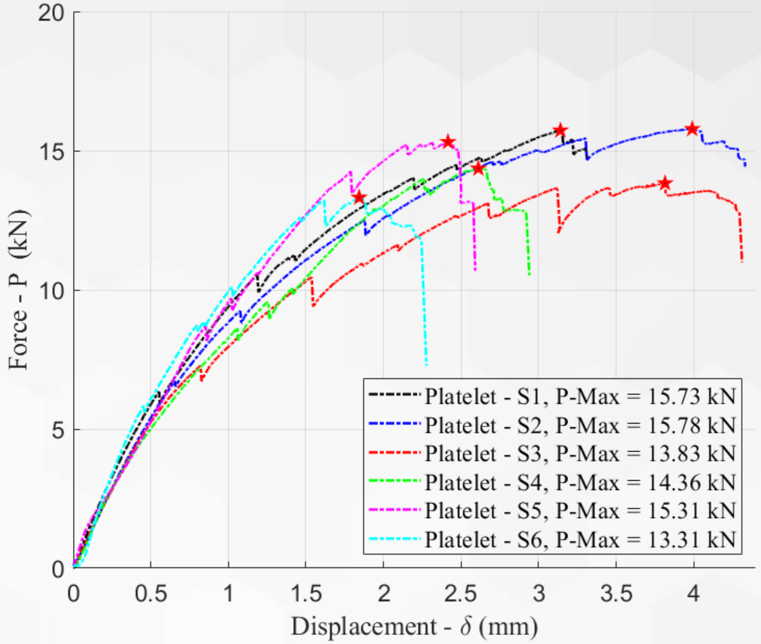

Pin Bracket Type	Average	Standard Deviation	Coefficient of Variance
Load - P (kN) @ Onset of Failure			
SMC	7.67	1.40	18.19%
CF & SMC	15.32	1.50	9.81%
Load - P (kN) @ Ultimate Failure			
SMC	14.72	1.04	7.05%
CF & SMC	18.38	1.10	6.01%

Acknowledgements

Composites Additive Manufacturing Group

Research Sponsors / Partners

NORTHROP GRUMMAN
The Composites Institute iacmi
BOEING
THERMWOOD LSAM Large Scale Additive Manufacturing
BELL
TECHMER PM POLYMER MODIFIERS
DASSAULT SYSTEMES
سابك sabic
LOCKHEED MARTIN
9T LABS
DUPONT
Dimensional Innovations

Thank You